




RESEARCH ARTICLE

THE EFFECT OF FIRING TEMPERATURE ON THE PROPERTIES OF GLAZES  
PREPARED WITH BARIUM-BASED FRIT

Betül YILDIZ<sup>1,\*</sup>

<sup>1</sup> Bilecik Şeyh Edebali University, Faculty of Engineering, Department of Metallurgical and Materials Engineering, Bilecik, Türkiye

[betul.yildiz@bilecik.edu.tr](mailto:betul.yildiz@bilecik.edu.tr) -  [0000-0002-7520-7722](https://orcid.org/0000-0002-7520-7722)

Abstract

Barium-based frits are commonly utilized in the ceramic tile industry to produce matte glazes. In these glazes, the microstructure—and consequently, the opacity and matte finish—vary depending on factors such as composition, application conditions, and firing temperatures. This study investigates the effects of different firing temperatures on the microstructure and properties of glazes prepared with barium-based frits. For this purpose, compositions containing 92 wt% barium-based frit and 8 wt% kaolin were milled, applied to the tile surface, and then fired in a laboratory furnace at four different peak temperatures (900, 1000, 1100, and 1200°C). The results indicate that the primary phase formed in the glaze structure is celsian at peak temperatures of 1100°C and 1200°C. As the temperature increases, the glassy phase expands, and crystal size increases. A decrease in the whiteness value ( $L^*$ ) value was observed with rising temperature; however, the glaze generally maintained its matte finish, as indicated by the 60° gloss value.

Keywords

Barium based frits,  
Ceramic glaze,  
Firing

Time Scale of Article

Received :08 November 2024  
Accepted : 12 December 2024  
Online date :27 December 2024

1. INTRODUCTION

Ceramic glazes are glassy coatings that improve the hygiene, functionality, and visual appeal of ceramic products [1,2]. Glazes are mixtures and glassy coatings created from finely ground ceramic raw materials, formulated with specific compositions. When fired onto the ceramic surface, they form a glass-like structure [3]. Standard glaze formulations consist of ceramic raw materials and various frits [4]. After grinding and applying the glaze to a ceramic body, it is fired to form a partially or fully vitreous coating. This glaze enhances both the chemical and mechanical properties of the ceramic substrate [5, 6]. In addition to these functional properties, glaze significantly contributes to the aesthetic qualities of ceramic tiles [1].

In the industrial sector, glazes are commonly categorized based on their optical characteristics into four groups: transparent matte, transparent glossy, opaque matte, and opaque glossy. Matte glazes tend to have greater surface roughness compared to glossy ones, which leads to multiple reflections of incoming light. This results in reduced specular reflection and a lower gloss level. The roughness observed in matte glazes is typically attributed to the presence of crystals. These crystals are thought to obstruct the smooth flow of the surface. Even in the absence of crystals, any glaze with high viscosity can create a matte finish due to insufficient surface smoothness [7, 8]. Common crystals observed in matte glazes include wollastonite ( $\text{CaSiO}_3$ ) and willemite ( $\text{Zn}_2\text{SiO}_4$ ) [9]. Alongside wollastonite- and willemite-based glazes, celsian ( $\text{BaAl}_2\text{Si}_2\text{O}_8$ ) based glazes which are used to achieve matte surfaces, have become popular in tile production. [7].

\*Corresponding Author: [betul.yildiz@bilecik.edu.tr](mailto:betul.yildiz@bilecik.edu.tr)

BaO functions as a flux in ceramic glazes and frits, though it becomes active at temperatures above 1100°C. Below this temperature, BaO promotes crystallization by increasing viscosity [5]. The addition of BaO enhances glaze brightness; improves mechanical properties, and lowers the thermal expansion coefficient [3, 8]. BaO is typically introduced into glaze compositions as BaCO<sub>3</sub>; however, due to its high toxicity, it is preferably incorporated through frits [5, 10, 11].

The microstructure of glazes generally consists of amorphous phase, porosity, and crystalline phase(s) [12]. The composition of ceramic glazes, grinding conditions, application parameters on tile surfaces, and firing schedules directly influence the microstructure and, consequently, the aesthetic, chemical, and technical properties of the glaze [13]. This research examines how different firing temperatures affect the microstructure and optical characteristics of glazes prepared with commercial barium-based frit.

Several studies have examined the effects of firing temperatures on glaze properties. Tezza et al., for instance, investigated how firing temperature influences the characteristics of anatase-based glazes [14], while Fröberg et al. explored the effects of composition and firing cycles on phase formation in raw glazes for floor tiles [15]. Imer et al. investigated the impact of firing temperatures on the structure of luster coatings [16]. Zhao et al. also explored how glaze composition and firing cycles affect the Raman polymerization index in celadon ceramic glazes [17]. Schabbach et al. analyzed the impact of peak firing temperatures on color development in zircon-based glazes [18].

In particular, Bou et al. investigated how firing temperatures affect the structure and aesthetic properties of barium-based glazes, with a focus on the influence of grain size distributions and firing temperatures on structure and mattiness in matte wall and floor tile glazes. Their study used high BaO-content barium frits for single-firing tile glazes and glazed porcelain tile production. These frits were mixed with raw materials such as zircon, nepheline, and feldspar, ground, and fired at various peak temperatures. After firing, zircon, celadon, and barium orthoclase phases were identified in the glazes. The glazes were fired at peak temperatures of 1000, 1020, 1040, 1060, and 1080°C, with observed decreases in L\* and gloss values as temperatures increased [7].

In the present study, commercial barium-based frit was similarly utilized, but with a broader range of firing temperatures compared to Bou et al.'s study. Additionally, to examine the effect of temperature solely on the frit structure, no raw material other than 8 wt% kaolin was incorporated into the glaze composition. The glazes were prepared using 92 wt% barium-based frit and 8 wt% kaolin, then fired at four different peak temperatures ranging from 900°C to 1200°C, with 100°C intervals, in a laboratory-scale furnace. The effects of varying firing temperatures on glaze microstructure and aesthetic properties were examined while other factors remained constant.

## **2. EXPERIMENTAL METHODS**

### **2.1. Preparation and Firing of Glaze Samples**

In this study, a glaze formulation was developed using a commercial frit composition. The chemical composition of the commercial frit is shown in Table 1. A glaze mixture consisting of 92 wt% barium-based frit and 8 wt% kaolin was placed into a mill with a solid-to-liquid ratio of 70%. Next, 0.2 wt% sodium carboxy methyl cellulose (CMC) and 0.2 wt% sodium tripolyphosphate (STPP) were incorporated, and the mixture was ground for 40 minutes. After milling, the glaze density was measured to be 1.80 g/cm<sup>3</sup>. A fluidity test conducted with a 4 mm Ford Cup showed a flow time of 18 seconds. The glaze suspensions were applied to the surface of wall tiles using a 0.8 mm glazing tool. The tiles were subsequently dried at 110°C for 30 minutes. Afterward, they were fired in a Nabertherm N210E laboratory furnace at four distinct peak temperatures. The samples were heated at a rate of 10°C/min until reaching their peak temperature, held at that temperature for 10 minutes, and then cooled back to

room temperature at the same rate. To assess the impact of different firing temperatures on the glaze, the samples were fired at peak temperatures of 900°C, 1000°C, 1100°C, and 1200°C. The corresponding sample codes and descriptions are provided in Table 2.

In a previous study, the melting behavior of this frit was analyzed using hot-stage microscopy, and the particle size distribution after 40 minutes of grinding was measured using a laser technique [13]. The relevant data are provided in Tables 3 and 4, respectively. After 40 minutes of grinding, the d(0.5) value of the glaze was determined to be 6.862  $\mu\text{m}$  (Table 3). The softening, half-sphere, and fusion temperatures of the glaze were found to be 854°C, 1156°C, and 1162°C, respectively. The glaze did not exhibit spherical behavior with increasing temperature (Table 4).

**Table 1.** The chemical composition of the frit coded as Ba-F [13]

Ba-Based Frit	Oxide weight %
Na <sub>2</sub> O	1-5
K <sub>2</sub> O	1-5
CaO	7-15
BaO	7-15
ZnO	7-15
Al <sub>2</sub> O <sub>3</sub>	10-18
B <sub>2</sub> O <sub>3</sub>	1-8
SiO <sub>2</sub>	45-55

**Table 2.** Samples' codes and explanation

Sample code	Explanation
Ba-F	Barium based commercial frit
S Glaze	Unfired raw glaze prepared with Ba-F
S-900	S glaze fired at 900°C
S-1000	S glaze fired at 1000°C
S-1100	S glaze fired at 1100°C
S-1200	S glaze fired at 1200°C

**Table 3.** Particle size distribution of S glaze after 40 minutes of grinding [13]

Sample	d(0.1)	d(0.5)	d(0.9)
S Glaze	1.553	6.862	26.761

**Table 4.** Results of hot stage microscopy analysis of S glaze after 40 minutes of grinding [13]

S Glaze	Temperature(°C)
T <sub>Sintering</sub>	852
T <sub>Softening</sub>	854
T <sub>Sphere</sub>	-
T <sub>Half Sphere</sub>	1156
T <sub>Fusion</sub>	1162

### **2.1.2 Glaze Characterization**

Panalytical/Empyrean diffractometer was used to determine the phases formed in the glaze structure after firing process. The glazed samples were analyzed within the  $2\theta$  range of  $10^\circ$  to  $90^\circ$ .

The microstructure of the glazed tiles was analyzed with a field emission scanning electron microscope (FE-SEM) equipped with an EDS detector (ZEISS, Gemini 500). Images were obtained from the cross-sectional surfaces of the glazes at magnifications of 500X and 1000X using a backscattered electron detector. EDX analysis was carried out on the light gray (crystalline phase) and dark gray (glassy phase) areas of the S-1200 coded sample, where the formed crystals were clearly visible.

The color and gloss of the samples (measured at a  $60^\circ$  angle) were evaluated using a Konica Minolta Spectrophotometer CM 600D. To ensure the reliability of the results, both color and gloss measurements were conducted three times, and the average values were calculated from the obtained data.

## **3. RESULTS AND DISCUSSIONS**

The XRD patterns of the glazes are given in Figure 1. According to the XRD results, sanidine ( $(K,Na)AlSi_3O_8$ ) was detected in the glazes fired at  $900^\circ\text{C}$  and  $1000^\circ\text{C}$ , whereas the primary phase observed at  $1100^\circ\text{C}$  and  $1200^\circ\text{C}$  was identified as celsian. Given that BaO behaves as an active flux above  $1100^\circ\text{C}$  [5], it is hypothesized that celsian crystal formation may have been promoted in the glazes fired at temperatures exceeding  $1100^\circ\text{C}$ . Although different temperatures for the crystallization of celsian in glass-ceramic structures have been reported, it is generally observed that these temperatures range from  $800^\circ\text{C}$  to  $1050^\circ\text{C}$ . In a study examining the BaO ratio in glass-ceramic glazes of the BAS ( $BaO-Al_2O_3-SiO_2$ ) system, the celsian crystallization temperature was found to be between  $808^\circ\text{C}$  and  $918^\circ\text{C}$  [19]. Another study determined the crystallization temperature of barium feldspar in a glass-ceramic glaze to be  $955.6^\circ\text{C}$  [20]. In a further study, the formation temperature of celsian crystals in the BAS glass-ceramic system was found to range from  $870^\circ\text{C}$  to  $1050^\circ\text{C}$  [21,22]. In this study, the XRD analysis conducted demonstrates that distinct celsian crystals form in glazes fired at  $1100^\circ\text{C}$  and  $1200^\circ\text{C}$  under laboratory conditions. However, firing at  $900^\circ\text{C}$  and  $1000^\circ\text{C}$  did not provide sufficient conditions for the formation of celsian crystals.

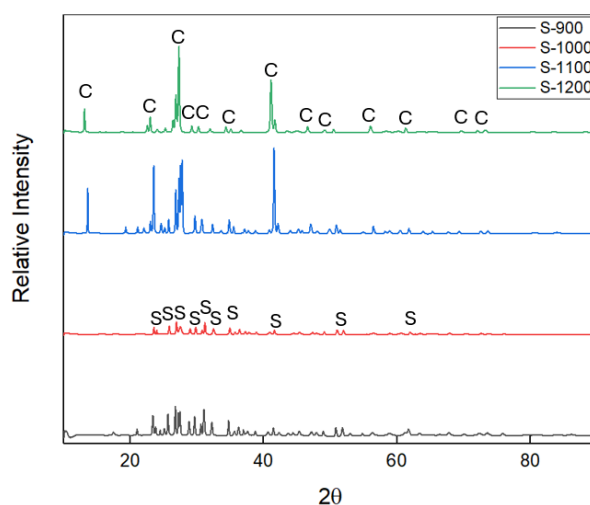


**Figure 1.** X-ray diffraction patterns of glazes (C: Celsian, S: Sanidine)

The microstructures of the glazed surfaces are given in Figure 2 and 3. In Figure 2, a noticeable decrease in the amount of porosity is observed as the temperature increases. The viscosity of the glaze decreased as the temperature increased during sintering [23]. Higher temperatures promoted the formation of more glassy phase, enhanced sintering and reduced the amount of porosity in the structure.

In the S-900 and S-1000 samples, sub micron crystals cluster are not clearly distinguishable within the glassy phase. However, as the temperature reaches 1100°C, the crystals within the glassy phase become more evident. In the S-1100 glaze, crystal sizes were observed to be below 10 microns, and the crystals formed a network-like structure in clusters. In contrast, in the S-1200-coded glaze, the width of the needle-like crystals ranged from 1 to 5  $\mu\text{m}$ , with lengths reaching up to 100  $\mu\text{m}$  (Figure 3). EDX analysis was performed on the S-1200-coded glaze. Figure 4 and Table 5 present the EDX patterns and elemental weight percentages determined for the glassy and crystalline phases of the S-1200 glaze. According to the EDX patterns, the intensities of the Al and Ba peaks from the dark area (glassy phase) were lower than those from the light area (crystalline phase), while the intensities of the Ca, Na, and Zn peaks were higher. The amount of barium element detected in the crystalline and glassy phases was 22.17% and 4.12%, respectively. These results demonstrate a clear correlation, indicating that the Ba content in the matrix crystallizes as celsian crystals. This finding is consistent with the XRD analysis, which further supports the observations.

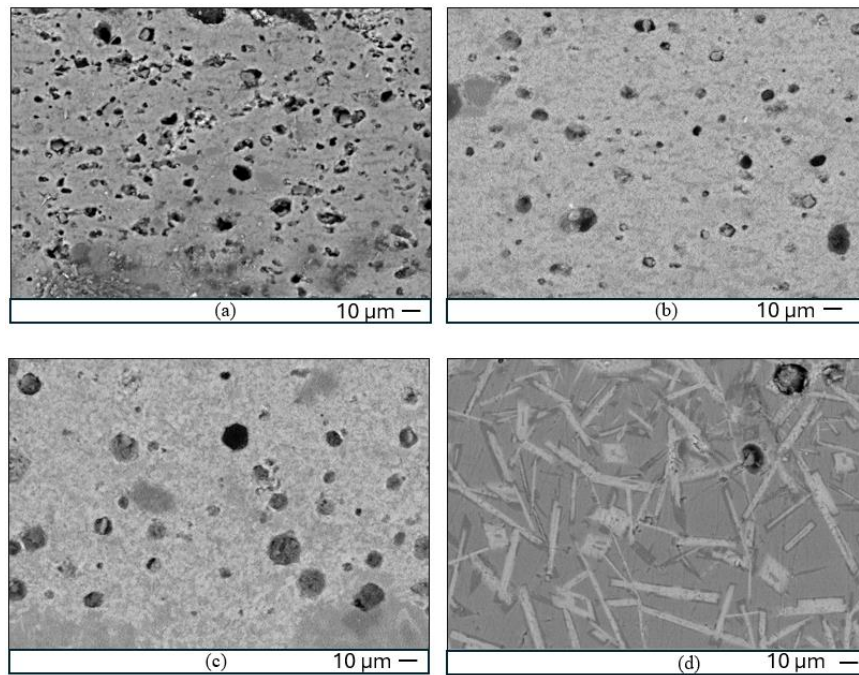


**Figure 2.** Scanning electron microscope images taken at 500x magnification using a backscattered electron detector from the cross-sectional surfaces of the studied glazes: (a) S-900; (b) S-1000; (c) S-1100; (d) S-1200.

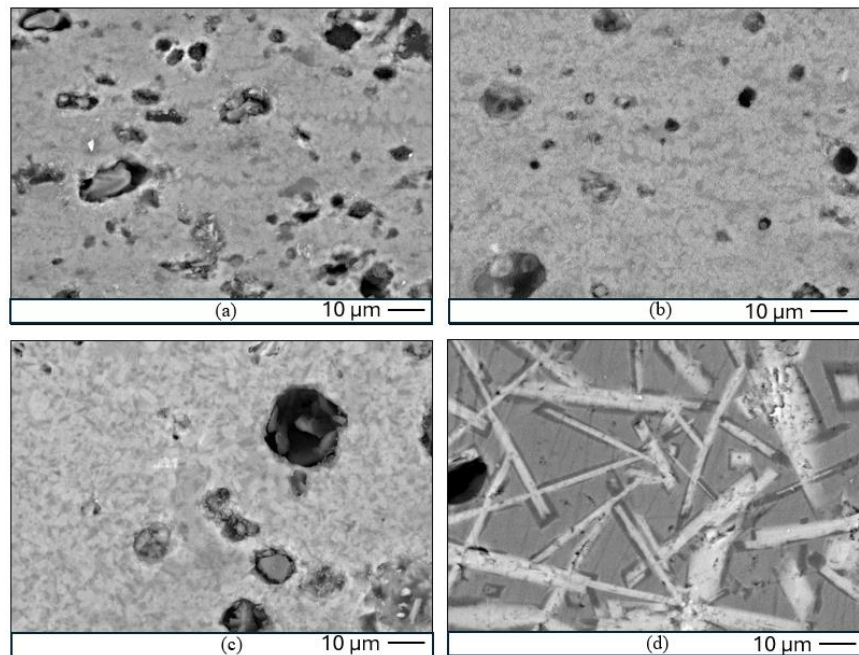


**Figure 3.** Scanning electron microscope images taken at 1000x magnification using a backscattered electron detector from the cross-sectional surfaces of the studied glazes: (a) S-900; (b) S-1000; (c) S-1100; (d) S-1200.

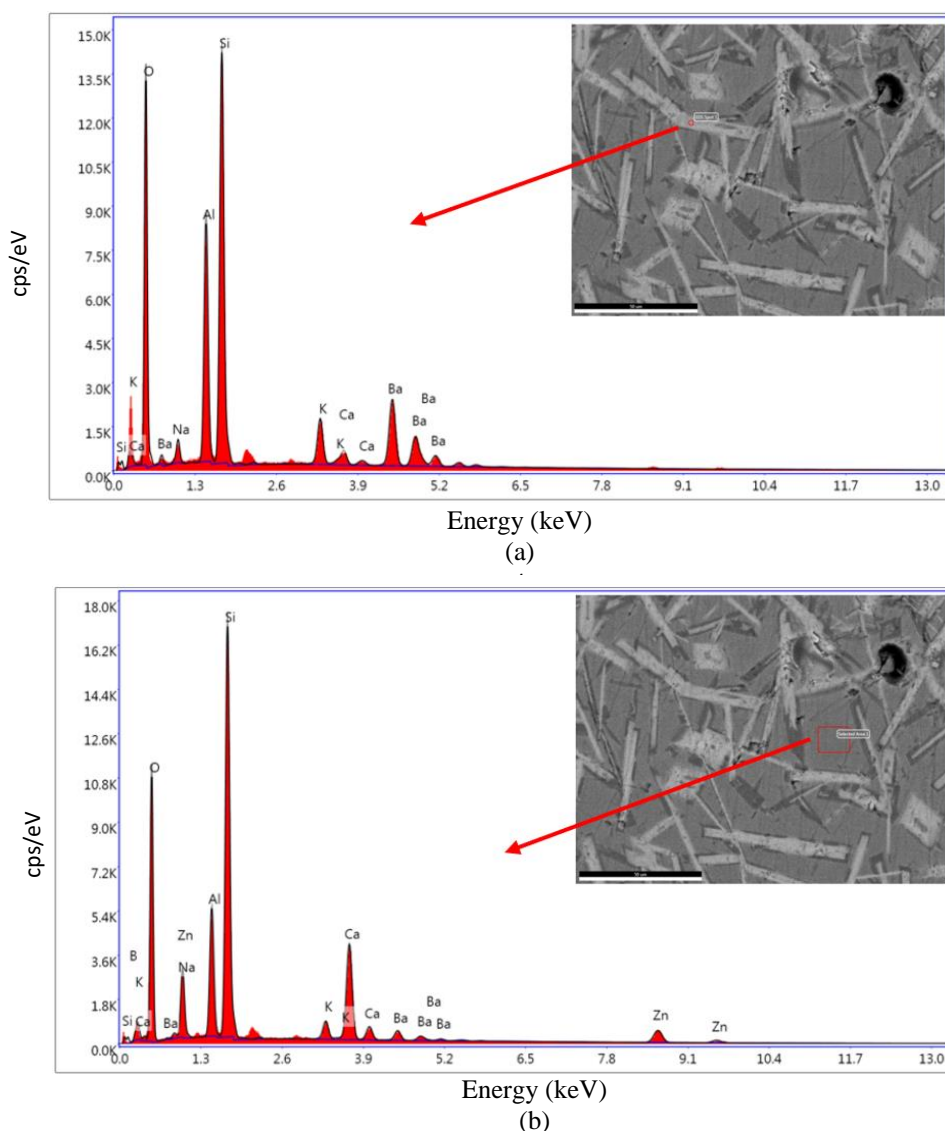


**Figure 4.** EDX pattern of the S-1200 coded glaze: (a) from the white area (crystalline phase); (b) from the black area (glassy phase).

**Table 5.** Element wt% measured in the glassy phase and crystal phase by FESEM-EDX

	Ba	Al	Si	O	Zn	B	Ca	K	Na
Crystal phase (a)	22.17	13.72	22.87	33.72	-	-	1.35	3.74	2.44
Glassy phase (b)	4.12	8.23	25.27	40.83	6.98	0.7	11.74	1.82	0.3

The images of the glazes before and after firing are presented in Figure 5, while the color values of the glazes after firing are shown in Figure 6. When the relevant glazes were examined, the samples with codes R-900 and R-1000 displayed an unfired glaze appearance. This outcome can be attributed to the high viscosity and porosity, which impeded sintering. The reduced densification led to the unfired matte appearance [24]. As the firing temperature rises, the  $L^*$  value of the glazes decreases, indicating a reduction in opacity. However, no linear change was observed in the  $a^*$  and  $b^*$  values (Fig.6). The transparency/opacity of the glaze depends on several factors, including the type(s) of crystalline phase(s)



within the vitreous phase, the refractive index, the particle size of the crystals, the concentration of the crystalline phase, the glaze thickness, and the refractive index contrast between the vitreous and crystalline phases [6]. The refractive index of celsian crystals ranges from 1.59 to 1.61 [25], which is close to that of the remaining glassy phase. As a result, low-opacity ceramic glazes with low L\* values were achieved in celsian-based glazes with S-1100 and S-1200 codes. Each glaze in the study exhibited a gloss value of less than 10 when measured at a 60° angle. The higher L\* values in the S-900 and S-1000 glazes can be attributed to their unfired appearance, as well as the increased light scattering due to porosity and surface roughness.

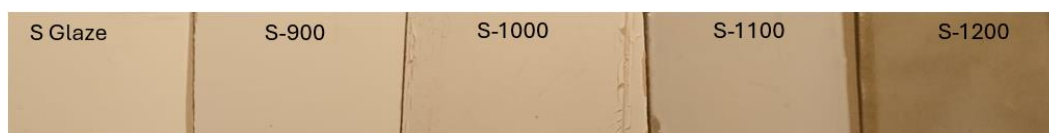


Figure 5. Visual appearance of the glazes

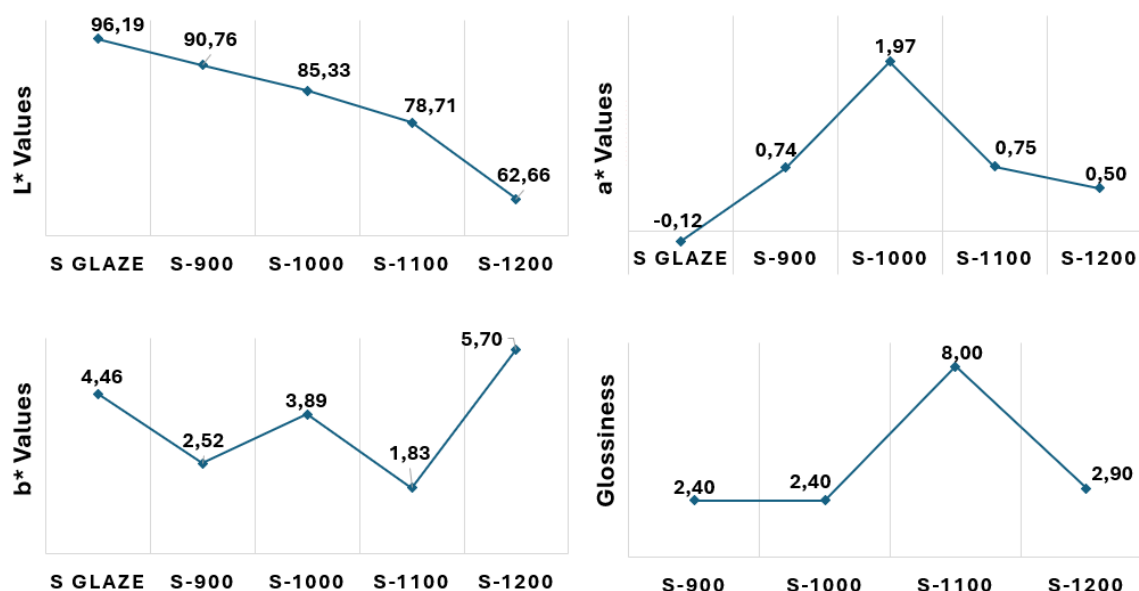


Figure 6. Variations in the color indices and glossiness values of the glazes

#### 4. CONCLUSIONS

This study investigates the effects of different firing temperatures on the glaze microstructure and color properties of barium-based frits. The findings are summarized as follows:

- With increasing firing temperature, the porosity of the glaze structure decreased, while the amount of the glassy phase increased. Celsian was the dominant phase in the S-1100 and S-1200 samples. As the temperature rose, the intensity of the celsian crystal peak within the glassy phase increased, and needle-like crystals formed, growing up to 100 microns.
- After firing at various temperatures, a matte opaque glaze with an appearance similar to an unfired glaze was obtained at 900°C and 1000°C, a satin opaque glaze at 1100°C, and a transparent matte glaze at 1200°C. The L\* value of the glaze decreased from 90.76 at 900°C to 62.66 at 1200°C.



- Considering that wall tiles are typically fired at temperatures between 1050°C and 1150°C, floor tiles between 1150°C and 1200°C, and porcelain tiles between 1200°C and 1210°C in the ceramic industry, it was observed that, depending on the composition and firing temperature, matte glazes with different optical properties can be obtained by using barium-based frits.
- Even at temperatures above 1200°C, the preservation of celsian crystals within the transparent glaze structure shows that celsian based glaze structures could be achieved in porcelain tile regime.

## **ACKNOWLEDGEMENTS**

The author gratefully acknowledges the material support provided by Akcoat İleri Kimyasal Kaplama Malzemeleri San. ve Tic. A.Ş.

## **CONFLICT OF INTEREST**

The author stated that there are no conflicts of interest regarding the publication of this article.

## **CRedit AUTHOR STATEMENT**

**Betül Yıldız:** Conceptualization, Methodology, Investigation, Formal analysis, Writing-original draft, Writing- Review&Editing

## **REFERENCES**

- [1] Casasola R, Rincon JMa, Romero M. Glass–ceramic glazes for ceramic tiles: a review. *J. Mater. Sci.*, 2012; 47, 553-582.
- [2] Kurama S, Gürkan, EA, Ozturk ZB, Karaca Y, Ubay E. Bazalt kesim atıklarının yer karosu mat sırlarda kullanım potansiyelinin araştırılması. *ESOGÜ Müh. Mim. Fakültesi Dergisi*, 2023; 31 (3), 816-825.
- [3] Ozturk ZB, Karaca Y, Ubay E. Enhancing thermal properties and surface quality of lappato glazed porcelain tiles through milling time optimization. *Journal of Thermal Analysis and Calorimetry*, 2024; 149, 7279-7287.
- [4] Yazırlı B, Sarı H, Kayacı K, Kara F. Effect of nucleating agent additions on gahnite based glass-ceramic glazes. *J. Eur. Ceram. Soc.*, 2024; 44, 3344-3351.
- [5] Eppler RA, Eppler DR. *Glazes and Glass Coatings*. The American Ceramic Society, Ohio, 2000.
- [6] Taylor JR, Bull AC. *Ceramic Glaze Technology*. Oxford: Pergamon Press, 1986.
- [7] Bou E, Bordes MC, Felhu C, Gazulla MF, Ferrer F, Pasiés G. Variables that determine the matt appearance of some ceramic floor and wall tile glazes. *Proceeding of VII world congress on ceramic tile quality Qualicer*, 2002; 349-364.
- [8] Campa F, Ginés F, Robles J. Matting of a transparent porous wall tile glaze by adding alumina. *Proceeding of VI world congress on ceramic tile quality Qualicer*, 2000; 115-117.
- [9] Kronberg T, Hupa L. The impact of wollastonite and dolomite on chemical durability of matte fast-fired raw glazes. *J. Eur. Ceram. Soc.*, 2020; 40, 3327-3337.

- [10] Fortuna D. Sanitaryware. Faenza: Gruppo Editoriale; 2000.
- [11] Stefanov S, Batschwarov S. Ceramic glazes. Bauverlag; 1988.
- [12] Sheikhattar M, Attar H, Sharafi S, Carty WM. Influence of surface crystallinity on the surface roughness of different ceramic glazes. *Materials Characterization*, 2016; 118, 570-574.
- [13] Yıldız B. Effect of particle size distribution on the properties of celsian based glazes. *Journal of Australian Ceramic Society*, 2024.
- [14] Tezza VB, Scarpato M, Oliveira LFS, Bernardin AM. Effect of firing temperature on the photocatalytic activity of anatase ceramic glazes. *Powder Technology*, 2015; 276, 60-65.
- [15] Fröberg L, Kronberg T, Hupa L, Hupa M. Influence of firing parameters on phase composition of raw glazes. *J. Eur. Ceram. Soc.*, 2007; 27, 1671-1675.
- [16] İmer C, Günay E, Öveçoğlu ML. Effects of firing temperatures and compositions on the formation of nano particles in lustre layers on a lead-alkali glaze. *Ceramics International*, 2016; 42, 17222-17228.
- [17] Zhao L, Zhang Y. Revealing the individual effects of firing temperature and chemical composition on raman parameters of celadon glaze. *Ceramics*, 2023; 6, 1263-1276.
- [18] Schab LM, Bondioli F, Ferrari AM, Manfredini T, Petter, CO, Fredel MC. Influence of firing temperature on the color developed by a (Zr,V)SiO<sub>4</sub> pigmented opaque ceramic glaze. *J. Eur. Ceram. Soc.*, 2007; 27, 179-184.
- [19] Altındal F, Anil UE, Varisli SO, Ozturk B. Investigation of the effect of BaO-Al<sub>2</sub>O<sub>3</sub> variations for BAS glass-ceramic glaze: Insights into thermal, phase, microstructural and surface features. *J. Eur. Ceram. Soc.*; 2024; 44, 3200-3209.
- [20] Partyka J, Lesniak M. Preparation of glass-ceramic glazes in the SiO<sub>2</sub>-Al<sub>2</sub>O<sub>3</sub>-CaO-MgO-K<sub>2</sub>O-Na<sub>2</sub>O-ZnO system by variable content of ZnO. *Ceram. Int.*, 2016; 42, 8513-8524.
- [21] Kaczmarczyk K, Partyka J. Effect of ZrSiO<sub>4</sub> addition on Sintering and selected physicochemical parameters of glass-ceramic materials from the SiO<sub>2</sub>-Al<sub>2</sub>O<sub>3</sub>-Na<sub>2</sub>O-K<sub>2</sub>O-CaO-MgO system in the presence of barium oxide. *Ceram. Int.*, 2019; 45, 22813-22820.
- [22] Han YX, Liu J, Yin WZ. Research on the mechanism of the dissociation of potassium shale during roasting. *Adv. Mater. Res.*, 2009; 58, 155-162.
- [23] Reinoso RR, Rubio-Marcos F, Solera E, Bengochea MA, Fernandez JF. Sintering behaviour of nanostructured glass-ceramic glazes. *Ceramics International*, 2010; 36, 1845-1850.
- [24] Suvaci E, Yıldız B. Roles of CaO, MgO and SiO<sub>2</sub> on crystallization and microstructure development in diopside-based glass-ceramic glazes under industrial fast firing condition. *J. Aust. Ceram. Soc.*, 2016.
- [25] Shannon RD, Shannon RC, Medenbach O, Fischer RX. Refractive index and dispersion of fluorides and oxides. *J. Phys. Chem. Ref. Data*, 2002; 31(4), 931-970.